THE ROYAL SOCIETY

Published online 2 May 2002

Self-organized instability in complex ecosystems

Ricard V. Solé[1,2*], David Alonso[1,3] and Alan McKane[4]

[1]*Complex Systems Research Group, Department of Physics, FEN-UPC Campus Nord B4, 08034 Barcelona, Spain*
[2]*Santa Fe Institute, 1399 Hyde Park Road, Santa Fe, NM 87501, USA*
[3]*Department of Ecology, Universitat de Barcelona, Diagonal 645, 08045 Barcelona, Spain*
[4]*Department of Theoretical Physics, University of Manchester, Manchester M13 9PL, UK*

Why are some ecosystems so rich, yet contain so many rare species? High species diversity, together with rarity, is a general trend in neotropical forests and coral reefs. However, the origin of such diversity and the consequences of food web complexity in both species abundances and temporal fluctuations are not well understood. Several regularities are observed in complex, multispecies ecosystems that suggest that these ecologies might be organized close to points of instability. We explore, in greater depth, a recent stochastic model of population dynamics that is shown to reproduce: (i) the scaling law linking species number and connectivity; (ii) the observed distributions of species abundance reported from field studies (showing long tails and thus a predominance of rare species); (iii) the complex fluctuations displayed by natural communities (including chaotic dynamics); and (iv) the species–area relations displayed by rainforest plots. It is conjectured that the conflict between the natural tendency towards higher diversity due to immigration, and the ecosystem level constraints derived from an increasing number of links, leaves the system poised at a critical boundary separating stable from unstable communities, where large fluctuations are expected to occur. We suggest that the patterns displayed by species-rich communities, including rarity, would result from such a spontaneous tendency towards instability.

Keywords: scaling; species-abundance distributions; rarity; species–area relations; spatial dynamics

1. INTRODUCTION

Diversity in complex ecosystems results from different processes operating on vastly different spatial and temporal scales. The patterns resulting from these processes provide different views of ecosystems: some populations fluctuate wildly on a scale of months or years but some large-scale features remain essentially unchanged in time. Together with unpredictable fluctuations, we see stable, macroscopic variables (such as biomass or productivity) that barely change over long time-scales. Understanding the nature of such fluctuations has important consequences and can reveal the underlying laws of ecosystem dynamics.

The biosphere is a complex adaptive system (Levin 1998). As such, it displays some universal features common to other far from equilibrium systems. In this context, beyond the plethora of fine-scale details present in any ecosystem, simple laws can account for well-defined macroscopic patterns (MacArthur & Wilson 1967; May 1974; Brown 1995; Maurer 1999).

A vast literature on model ecosystems has been accumulating over the past few decades (May 1974; Pimm 1991; Ricklefs & Schulter 1993; Morin 1999) together with an increasing understanding of how real ecologies are organized. This constantly improving picture becomes more and more important as we start to realize that our biosphere is actually experiencing a mass extinction event of as yet unknown consequences (Leakey & Lewin 1996; Levin 1999). Any useful forecast of future diversity losses will need the support of *model* ecosystems. It is not possible to obtain detailed knowledge of even moderately diverse biotas (not to mention the most endangered and rich ones), but if strong regularities can be identified and reproduced by simple, yet reasonably accurate, models then we can hope to provide some real understanding of how ecosystems emerge and how fragile they are.

Most of the available literature on multispecies communities considers only one aspect of the whole picture. Some analyse the dynamics of an ecological time-series and its possible origins (Schaffer 1984; Ellner & Turchin 1995; Turchin & Ellner 1998; Gamarra & Solé 2000). Others explore the statistical regularities present in mature communities, such as the type of species–abundance relations (May 1975; Brown 1995; Maurer 1999) exhibited by different types of community. A number of structural regularities have also been identified concerning the patterns of links among species, involving both the topology of the underlying graph (Paine 1966; Pimm 1991; Williams & Martinez 2000; Montoya & Solé 2002*a*,*b*) and the patterns of interaction strengths (McCann *et al.* 1998). Finally, one of most celebrated laws in ecology is the so-called SAR: the number of species S found in a particular area increases with the area size A as a power law: $S = \eta A^z$, where η is a constant and z a characteristic exponent. Most models explore the possible origins of these four properties by considering them in isolation. As

*Author and address for correspondence: Santa Fe Institute, 1399 Hyde Park Road, Santa Fe, NM 87501, USA (sole@santafe.edu).

One contribution of 11 to a special Theme Issue 'The biosphere as a complex adaptive system'.

a consequence, fairly different mechanisms can account for the same regularities. This is a rather unsatisfactory situation, since an appropriate understanding of ecological patterns should involve all of them: the statistical patterns are the outcome of underlying dynamical processes and a link between them should be properly established.

We present a unified view of how complex ecosystems become organized, involving all the previous aspects within the same framework. A previous theoretical model (McKane *et al.* 2000; Solé *et al.* 2000) is used as a starting point. This model approach is based on a stochastic interacting particle system (Durrett & Levin 1994; Durrett 1999) involving a community assembly process in time and space (Drake 1990*a*,*b*). We propose that the observed regularities common to a large number of ecological systems originate from the conflict between increasing diversity (due to immigration or speciation) and decreasing species richness, derived from increasing levels of interaction.

This paper is organized as follows. In § 2 we summarize some of the main regularities exhibited by real ecosystems and the corresponding theoretical interpretations. In § 3 the two basic models are introduced and in § 4 the time evolution of these models and the resulting final stationary species–connectivity relations are presented, together with our basic hypothesis. The spatial extension of the spatially implicit models of § 3 is provided in § 5, where its SAR is studied using numerical simulations. Our results, their fit with real data and their possible implications are outlined in § 6.

2. REGULARITIES IN REAL ECOSYSTEMS

(a) *Stability and complexity*

The quest for stability in real ecosystems has been traditionally linked with species diversity (McCann (2000) and references therein). Arguments emerged suggesting that stability is either reinforced (Odum 1953; Elton 1958) or jeopardized (May 1972, 1974) by diversity. Early rigorous theoretical studies explore the problem of stability under the light of *linear* stability analyses (May 1974). In those models, interactions among species are described through Lotka–Volterra equations, i.e. a set of S differential equations:

$$\frac{\mathrm{d}N_i}{\mathrm{d}t} = \Phi_i(\boldsymbol{N}) = N_i(t)\left(\epsilon_i - \sum_{j=1}^{n} \alpha_{ij} N_j(t)\right), \tag{2.1}$$

where $\{N_i\}$; $(i = 1,\ldots,S)$ is the population size of each species. Here ϵ_i and α_{ij} are constants that introduce feedback loops and interactions among different species. The community matrix $\boldsymbol{A} = (\alpha_{ij})$ is assumed to have a connectivity $C \in [0,1]$, defined as the fraction of nonzero elements in $\boldsymbol{A}$. Linear stability studies of these models assumed that there was an equilibrium state $\boldsymbol{N}^*$, such that $\Phi_i(\boldsymbol{N}^*) = 0$ and the system was considered unstable if small deviations from $\boldsymbol{N}^*$ were amplified under this approximation.

One of the most important results obtained from these models was a formal relation between stability and complexity in model random ecosystems (May 1974). In short, using Lotka–Volterra equations with random links among species, May found that the probability of an S-species ecosystem being stable, $P(S,\alpha,C)$, displays a threshold behaviour of the following kind:

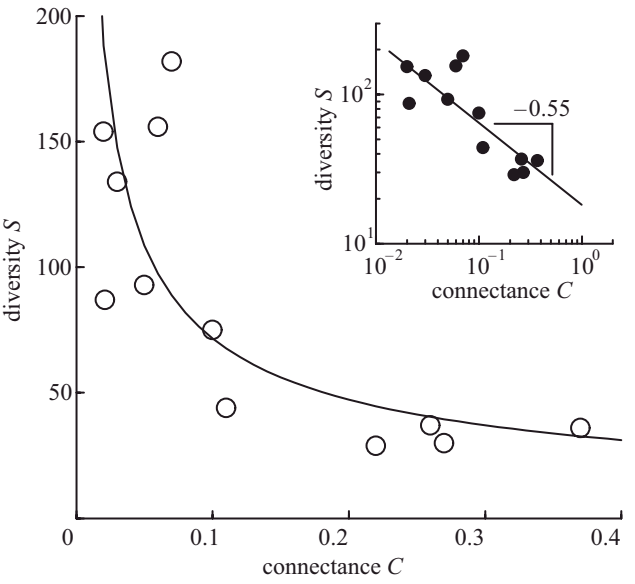

Figure 1. Scaling relation between diversity (number of species, S) and complexity (measured in terms of the connectance, C). The data were obtained from 12 well-defined ecological networks (Montoya & Solé (2002*b*) and references therein). The observed exponent (inset, log–log plot of the same data) strongly deviates from the standard $S \propto C^{-1}$ hyperbolic law.

if $\alpha^2 SC < 1$ then $P(S,\alpha,C) \to 1$ as $S \to \infty$,

if $\alpha^2 SC > 1$ then $P(S,\alpha,C) \to 0$ as $S \to \infty$.

Thus, a limit to species diversity is imposed by the critical boundary $\alpha^2 SC = 1$. The first field tests of this theory confirmed the presence of a scaling law between diversity and connectivity, as predicted. In addition, this law was also found to be present in more realistic models (Pimm 1982) and has motivated many studies (Winemiller 1990; Polis 1991; Martinez 1992, 1994; Reagan & Wade 1996; Montoya & Solé 2002*b*). Further re-analysis of model networks with some amount of hierarchical structure revealed that a scaling law was present but allowed the stabilization of a larger number of species (Hogg *et al.* 1989).

Further detailed analyses of real food webs demonstrated that, in fact, the actual scaling law should be written as

$$S \propto C^{-1+\epsilon} \tag{2.2}$$

where $\epsilon \in [0, 1/2]$ (figure 1). This is an important deviation from the predicted hyperbolic law $S \propto C^{-1}$. But what is perhaps more interesting is the fact that the S–C diagram suggests that all the observed systems seem to follow a scaling relation. If collective community stability were a global property to be optimized, one should expect to find points scattered throughout the lower part of the diagram. This is not the case. Why?

(b) *Species–abundance relations*

The second ingredient in the ecological theory of complex ecosystems is provided by species–abundance distributions (Pielou 1969; May 1975; Hubbell 1979; Pachepsky *et al.* 2001). These distributions provide a stat-

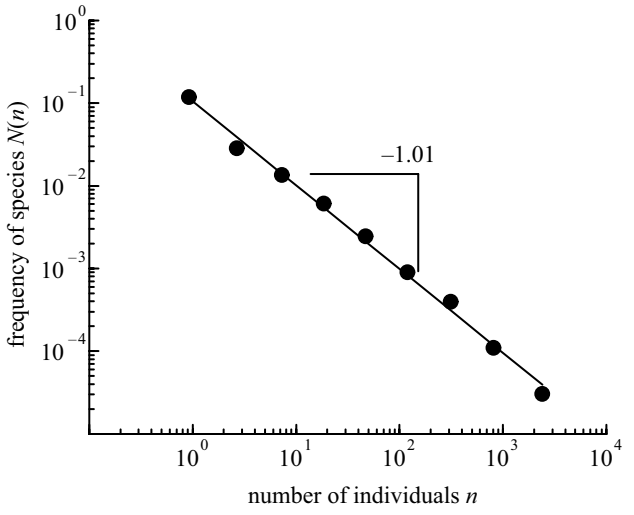

Figure 2. Power-law distribution of Mediterranean diatoms. Margalef (1994) offers an ensemble inventory of phytoplankton by putting together more than 2000 samples. This includes 1 045 830 identified cells. Data obtained from Pueyo (2002).

istical view of the whole community in terms of the relative abundances of the different species. Species–abundance distributions involve the number of species $S(n)$ represented by n individuals. Obviously, the total number of species S and the number of individuals N are obtained from $S(n)$ through

$$S = \int_0^\infty S(n)\mathrm{d}n, \tag{2.3}$$

$$N = \int_0^\infty nS(n)\mathrm{d}n, \tag{2.4}$$

where we have assumed that $S(n)$ is given by a continuous distribution. In spite of the potentially large number of observable distributions, a few of them are ubiquitous: the lognormal, the log series and the power laws. They share a common trait: they display long tails indicating that a few species are rather common and most are rare. The long-tailed distributions displayed by real ecologies have been interpreted in terms of stochastic multiplicative processes governed by the conjunction of a variable number of independent factors (May 1975). The power-law distributions can be considered a limiting case of the lognormal behaviour, and are observed in a number of ecological scenarios, from rainforests to marine ecosystems (figure 2).

These types of distribution are commonly found in a number of situations, including, for example, multiplicative processes (May 1975), coagulation–fragmentation models (Camacho & Solé 2000), coherent noise (Sneppen & Newman 1997) and in systems with interacting units having a complex internal structure (Amaral *et al.* 1998). In physics they are found at critical points (Binney *et al.* 1993; Solé *et al.* 1996, 1999; Stanley *et al.* 1996). Possible candidates in population biology are found in the spread of epidemics (Rhodes & Anderson 1996) and in the distribution of forest fires (Malamud *et al.* 1998). In this context, it has been suggested that the presence of power laws might indicate that the systems have self-organized themselves into a critical state (Bak *et al.* 1987). Self-organized critical systems require a number of strong constraints in order to operate (Jensen 1998), and it is not clear whether such constraints can operate in a broad range of situations (Solé *et al.* 1999; Solé & Goodwin 2001). However, partially inspired by ideas of this kind, we propose a mechanism of ecosystem organization in which the observed patterns result from the spontaneous driving of complex ecologies towards the marginal instability boundary defined by the *S–C* relation.

(c) *Fluctuations and chaos*

The use of linear stability analysis in this context has a number of drawbacks. The main one is of course the fact that real populations are far from equilibrium (Hastings *et al.* 1993; Ario & Pimm 1995). Complex fluctuations are found in most species that have a characteristic lifespan, and allow dynamical changes to be tracked as time evolves. Fluctuations can be highly variable, and in some cases have been identified as evidence of deterministic chaos (Schaffer 1985; Gamarra & Solé 2000). An interesting result, in our context, is the observation by Ellner & Turchin (1995) of a characteristic trend exhibited by many field and laboratory populations: when measuring the largest Lyapunov exponent from these time-series, λ_L, it was found to be clustered around zero (Ellner & Turchin 1995). The exponent λ_L gives a quantitative estimate of the degree of divergence of two initially close points in phase space (here defined in terms of the underlying populations) and thus is a measure of chaos. If $\lambda_L < 0$ then two trajectories will approach with time. If $\lambda_L > 0$, sensitive dependence will be present and thus chaotic dynamics. The critical point $\lambda_L^c = 0$ defines the boundaries between the two qualitative dynamical regimes. The fact that it is close to zero seems to support the idea that these systems might be close to that boundary.

3. STOCHASTIC MULTISPECIES MODELS

Many different types of mathematical and computer model of multispecies ecosystems have been developed over recent decades. One particularly useful approach is provided by SCA, also called interacting particle systems (Durrett & Levin 1994; Marro & Dickman 1999). In SCA, an individual-based description of the units is introduced at the simplest level. Several specific types of SCA have played a major role in physics, chemistry and biology. Examples are contact processes (Durrett & Levin 1994; Levin 1999) or the FFM (Bak *et al.* 1990; Drossel & Schwabl 1992). These models can be spatially implicit or explicit. In the first case, global population mixing is assumed, while in the second interactions occur on a given spatial domain and are local in nature. SCA have been widely used in theoretical ecology. Null models involving simple particle interactions have been shown to be very useful in providing insight into biodiversity dynamics (Alonso & Solé 2000; Hubbell 2001).

The following two models involve a discrete definition of individuals belonging to a given set of species. The dynamics is essentially probabilistic at the microscopic scale, but it leads to recognizable macroscopic patterns both in space (see below) and time.

(a) *Model A*

In two recent papers (McKane *et al.* 2000; Solé *et al.* 2000) we have proposed a simple model of species interactions that has been shown to display several of the statistical properties previously mentioned (hereafter model A). It corresponds to a generalization of Wright's model (Wright 1931; Hubbell 1979). The basic model is a mean-field (spatially implicit) interacting particle system (Durrett & Levin 1994; Durrett 1999). A system involving N individuals is considered, together with a pool $\Sigma(S)$ of S possible species. In particular, individuals belonging to different species could share exactly the same life-history traits. Thus, this modelling approach can also simulate neutral models (Bell 2000, 2001). This set-up can be understood in terms of a given area of a rainforest with a finite number of sites that is invaded by individuals from an outside pool. Interactions among individuals are introduced through a random matrix Ω. This matrix is fixed and has a predefined connectivity C. Two basic rules are defined.

(i) Immigration: a randomly chosen site occupied by species B is replaced by a species randomly chosen from the species pool, i.e. $A \in \Sigma(S)$:

$$B \xrightarrow{\mu} A. \tag{3.1}$$

This occurs with a probability (of immigration) μ.

(ii) Interaction: two randomly chosen individuals belonging to species $A,B \in \Sigma(S) - \{0\}$ will interact if $\Omega_{AB} \neq \Omega_{BA}$ (in particular this includes the case of no interaction). The result of the interaction will be

$$A + B \xrightarrow{\Omega} 2A, \tag{3.2}$$

if $\Omega_{AB} > \Omega_{BA}$ (and $A + B \rightarrow 2B$ otherwise).

(b) *Model B*

The previous model has been shown to be able to reproduce a broad number of basic, well-known field observations (McKane *et al.* 2000; Solé *et al.* 2000). However, the mechanisms of interaction used are too abstract and do not allow, in particular, the expansion of isolated species into empty sites. The second model again involves a set of S (possible) species plus empty sites (pseudospecies labelled 0). This set (the species pool) $\Sigma(S)$ is then a discrete set:

$$\Sigma(S) = \{0,1,2,\ldots,S\}, \tag{3.3}$$

where 0 indicates empty space, available to all species from the pool. Three basic types of transition are allowed to occur. Let us call $A,B \in \Sigma(S)$ two given species present at a given step. These possible transitions are summarized as follows.

(i) Immigration: an empty site is occupied by a species randomly chosen from the set of (non-empty) species, i.e. $A \in \Sigma(S) - \{0\}$:

$$0 \xrightarrow{\mu_i} A. \tag{3.4}$$

This occurs with a probability of colonization (of empty sites) μ_i. Notice that this colonization depends on the particular species.

(ii) Death: All occupied sites can become empty with some fixed probability e_i:

$$A \xrightarrow{e_i} 0. \tag{3.5}$$

(iii) Interaction: the same rule as in model A is used, but here the probability of success P_{ij} is weighted by the coefficients of the interaction matrix. Here we use

$$P_{ij} = \pi[\Omega_{ij} - \Omega_{ji}], \tag{3.6}$$

where $\pi[x] = x$ when $x > 0$ and zero otherwise. This probability of an interaction occurring in the system between species i and j is a measure of the interaction strength linking interacting species.

In other words, the parameters defining the interactions, colonization and extinction of species in model B are given by two vectors,

$$\boldsymbol{\mu} = (\mu_0,\mu_1,\ldots,\mu_S), \tag{3.7}$$

$$\boldsymbol{e} = (e_0,e_1,\ldots,e_S), \tag{3.8}$$

the immigration and the extinction vectors respectively, where here $\mu_0 = e_0 = 0$, and an $(S + 1) \times (S + 1)$ matrix Ω, which is such that $\Omega_{0i} = 0$ for all $i \in \Sigma(S) - \{0\}$. Additional rules (such as the presence of trade-offs between colonization and competition) can be easily introduced. Several variations of the previous models have shown the same basic patterns.

This model allows the simulation (as particular cases) of a number of well-known problems. Let us mention five of them.

(i) The predator–prey model (here empty sites, prey (1) and predators (2) are considered) would be represented as $\mu = (0,\mu_1,\mu_2)$, $\boldsymbol{e} = (0,e_1e_2)$ and the interaction matrix would be

$$\Omega = \begin{pmatrix} 0 & 0 & 0 \\ \Omega_{10} & 0 & 0 \\ 0 & \Omega_{21} & 0 \end{pmatrix}. \tag{3.9}$$

(ii) The contact process would include only two types of particle, active and inactive (exposed and infective), with $\mu = (0,0)$, $\boldsymbol{e} = (0,e_1)$ and the interaction matrix would be

$$\Omega = \begin{pmatrix} 0 & 0 \\ \Omega_{10} & 0 \end{pmatrix}, \tag{3.10}$$

where Ω_{10} corresponds to the infection rate and e_1 the recovery rate.

(iii) The FFM. Here the three states correspond to ashes: (empty sites), green trees (1) and burning trees (2). Two different types of model have been considered: the BCT version and the DS version. The only difference between them is that the second allows for the spontaneous burning of green trees. Now we have: $\mu = (0,\mu_1,\mu_2)$, $\boldsymbol{e} = (0,0,1)$, with $\mu_2 = 0$ in BCT and $\mu_2 \neq 0$ in the DS model. The interaction matrix is

$$\Omega = \begin{pmatrix} 0 & 0 & 0 \\ 0 & 0 & 0 \\ 0 & 1 & 0 \end{pmatrix}. \tag{3.11}$$

(iv) The model of Tilman (1994) addresses the question of the coexistence of a large number of species in hierarchical competitive communities. In this model, species i can colonize sites which are not occupied by superior competitors, but is extinguished from any site invaded by superior competitors. The model involves the proportion of sites occupied by species i (p_i), species-specific colonization rates (c_i) and mortality rates (e_i). The equation for species i is

$$\frac{\mathrm{d}p_i}{\mathrm{d}t} = c_i p_i \left(1 - \sum_{j=1}^{i} p_j\right) - e_i p_i - \sum_{j=1}^{i-1} c_j p_j p_i. \tag{3.12}$$

The stochastic counterpart of the deterministic model described by equation (3.12) can also be rewritten as a particular case of the stochastic model B, assuming no external immigration and with the extinction vector being $\boldsymbol{e} = (0, e_1, \ldots, e_{S-1}, e_S)$. Notice how the interaction matrix captures the hierarchical structure of the competitive community:

$$\Omega = \begin{pmatrix} 0 & 0 & \cdots & \cdots & \cdots & \cdots & 0 \\ c_1 & 0 & c_1 & \cdots & \cdots & \cdots & c_1 \\ \vdots & \vdots & \ddots & \ddots & \cdots & \cdots & \vdots \\ c_i & 0 & \cdots & 0 & c_i & \cdots & c_i \\ \vdots & \vdots & \vdots & \vdots & \ddots & \ddots & \vdots \\ c_{S-1} & 0 & \cdots & 0 & \cdots & 0 & c_{S-1} \\ c_S & 0 & \cdots & 0 & \cdots & 0 & 0 \end{pmatrix}. \tag{3.13}$$

A later version of the model (Tilman *et al.* 1994), introduced a habitat destruction parameter, D, which allowed the investigation of how habitat destruction causes species extinction.

(v) Hubbell's neutral theory of biodiversity (Hubbell 2001) is also based on a stochastic model that can be formalized as a particular case of model B. The colonization vector must now be defined as $\mu = (\mu_0, \mu_1, \ldots, \mu_S)$, where μ_0 is the perturbation rate, i.e. the probability of formation of a new gap in a lattice site per time unit. The matrix Ω takes into account only the ability of species to colonize empty space, and therefore has the same entries for all species. Species only differ in the immigration rate (μ_i) from an external biogeographic pool. Internal colonization of empty sites takes place in a way that is proportional to the relative abundance of any particular species in the lattice. Therefore, the matrix Ω is written as

$$\Omega = \begin{pmatrix} 0 & \cdots & \cdots & 0 \\ c & 0 & \cdots & 0 \\ \vdots & \vdots & \ddots & \vdots \\ c & 0 & \cdots & 0 \end{pmatrix}. \tag{3.14}$$

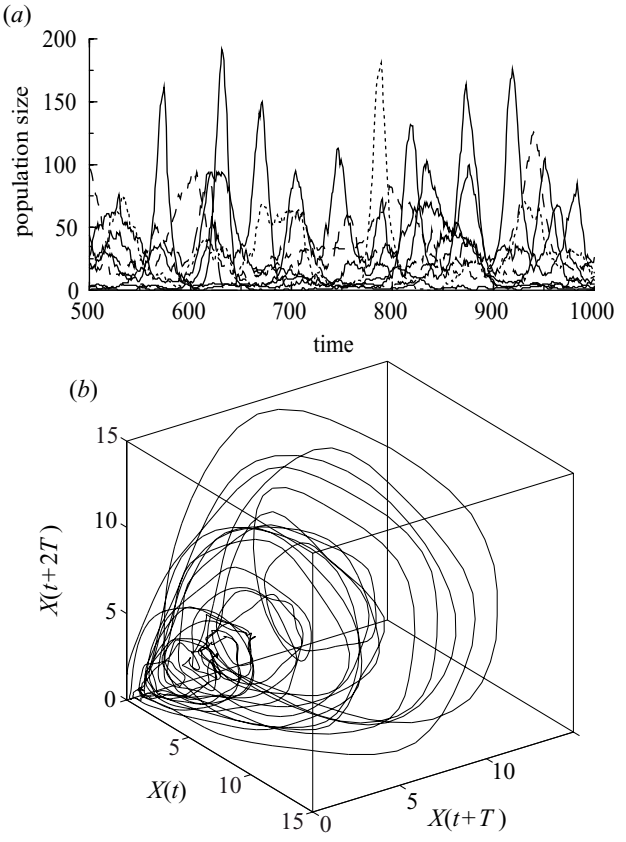

Figure 3. An example of the time-series obtained from the stochastic multiparticle model. (*a*) Fluctuations for different species (here $S = 30$, $N = 1000$, $\mu = 0.01$ and $C = 0.2$). (*b*) Reconstructed attractor for one of the previous time-series.

In Hubbell's model, extinction takes place as a result of an external perturbation. There are no species-specific mortality rates. Therefore, the extinction vector $\boldsymbol{e} = (e_0, e_1, \ldots, e_S)$ must be defined as a null vector.

The fact that these models exhibit a wide range of dynamical patterns (from spiral waves and chaos to self-organized critical behaviour) is important here. This wide range of patterns validates our choice of a model in which mechanisms of different kinds (which can create conflicting constraints of different types) are explicitly included.

4. TIME EVOLUTION AND STEADY-STATE PROPERTIES

(a) *Time-series analysis*

The first set of properties to be analysed are dynamic. As reported in a previous analysis (Solé *et al.* 2000) complex fluctuations are a common trait of model A. They are also common (and exhibit the same basic features) in model B. An example is shown in figure 3, where a small-species system ($S = 30$) has been used. Complex dynamical patterns are observable and in some cases they can be identified as deterministic chaos (Gamarra & Solé 2000; Turchin & Ellner 1998). In figure 3*b* we plot the reconstructed attractor obtained from one of the species time-series. Using standard techniques of time-series analysis (Ellner 1988) it can be shown, for this particular case, that a low-dimensional strange attractor is present, with a

fractal dimension $D_f = 3.32 \pm 0.12$. In general, small systems with high connectivities display this type of deterministic behaviour. This is not surprising since, under these conditions, we are actually simulating small-species systems under an individual-based approach. As the number of species increases or the connectivity becomes too small, the observed dynamics becomes much more irregular and no low-dimensional patterns are observed. In fact, the pattern of fluctuations displayed by these models under low connectivities, or high immigration, are consistent with a random-walk-like behaviour. It is important to note that these differences are not present in other neutral models, where the time-dependent dynamics exhibited by the populations are always high dimensional.

A link between dynamics and statistical features can easily be established by looking at the time evolution of the species–rank distributions. This type of pattern displayed by ecological succession has been studied in a number of well-known field studies (Bazzaz 1975; Hubbell 1979, 2001). This is displayed in figure 4, where the evolution of these distributions is shown for both models using $\mu = 0.01$, $C = 0.1$, $N = 4 \times 10^3$ and a pool involving $S = 400$ species. At $T \approx 600$ a stationary distribution is observed (although species replacement takes place all the time at the right-side of the curve). Both models behave in a similar way, except for the eventual more limited diversity achieved by model B. This is not surprising, since empty spaces are more likely to be occupied by the most common species already present.

A different aspect that can be studied in relation to temporal patterns is the presence of scaling in time fluctuations. The presence of scaling in natural populations has been shown not only in year-to-year population variability (Ariño & Pimm 1995) but also in lifetime distributions (Keitt & Stanley 1998). Specifically, these authors find that the lifetime distribution $P(T)$ of local populations scales as $P(T) \approx T^{-\theta}$ with $\theta \approx 1.6$ (Keitt & Stanley 1998). The previous stochastic lattice model also shows this kind of scaling property. In particular, using model B, lifetime distributions clearly look long-tailed (figure 5), with scaling exponents that depend on the parameters of the models, but that typically take a value $\theta \approx 1.5$ for large enough interaction rates. The behaviour for model A is slightly different: at low interaction rates, it shows random-walk behaviour, $\theta \approx 1.5$, but when C increases, it shows deviations from this quantity and moves towards $\theta \approx 1.0$. The lower values seem to be consistent with the analysis by Keitt and Marquet of the extinction patterns displayed by the Hawaiian avifauna, for which they found $\theta \approx 1$ (Keitt & Marquet 1996), although the statistical significance of their results might be small.

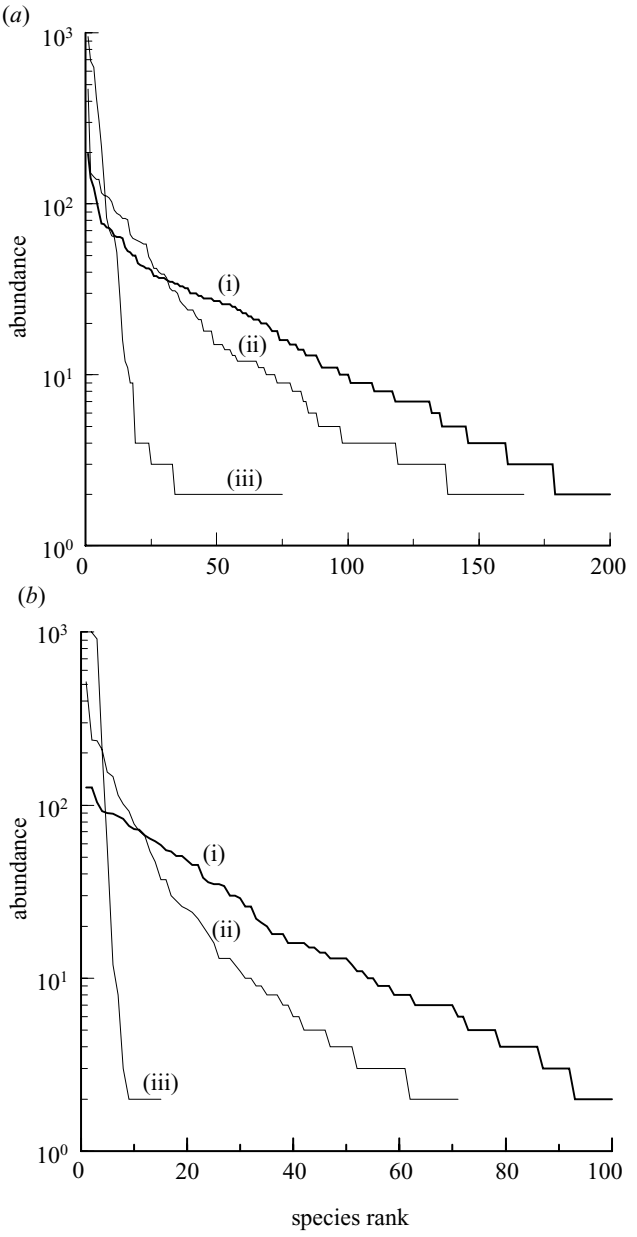

Figure 4. Time evolution of the species–rank distributions for models A and B. We start with an initial condition where only two species are present. Both models behave similarly, except for a smaller number of species being stabilized in model B. (i) $T = 600$; (ii) $T = 250$; (iii) $T = 50$.

(b) *Stationary distributions: mean field model*

In order to obtain the expected asymptotic species–abundance distributions, we can use model A and obtain $P(n)$ analytically, using a so-called *mean field* approximation. The mean field approximation considers a single, average species (which is characterized by some average properties) and the rest of the species defines a homogeneous, separated set. In some sense all species are considered equivalent and the fluctuations of this average species can be analysed exactly. Of course, the mean field approach does not take account of any correlations implicit in the matrix structure, but it can provide an appropriate quantitative characterization when such correlations are not very strong.

In order to obtain the stationary distribution of species–abundance, we can consider the one-step birth and death process (a particular class of Markovian processes) where only single-unit changes are allowed. Let us start with the master equation for this model. If $P(n,t)$ is the probability (for any species) of having n individuals at time t, the one-step process is described by (van Kampen 1981; Renshaw 1991)

$$\frac{\mathrm{d}P(n,t)}{\mathrm{d}t} = r_{n+1}P(n+1,t) + g_{n-1}P(n-1,t) - (r_n + g_n)P(n,t), \tag{4.1}$$

where $r_n \equiv W(n-1|n)$ and $g_n \equiv W(n+1|n)$ are the tran-

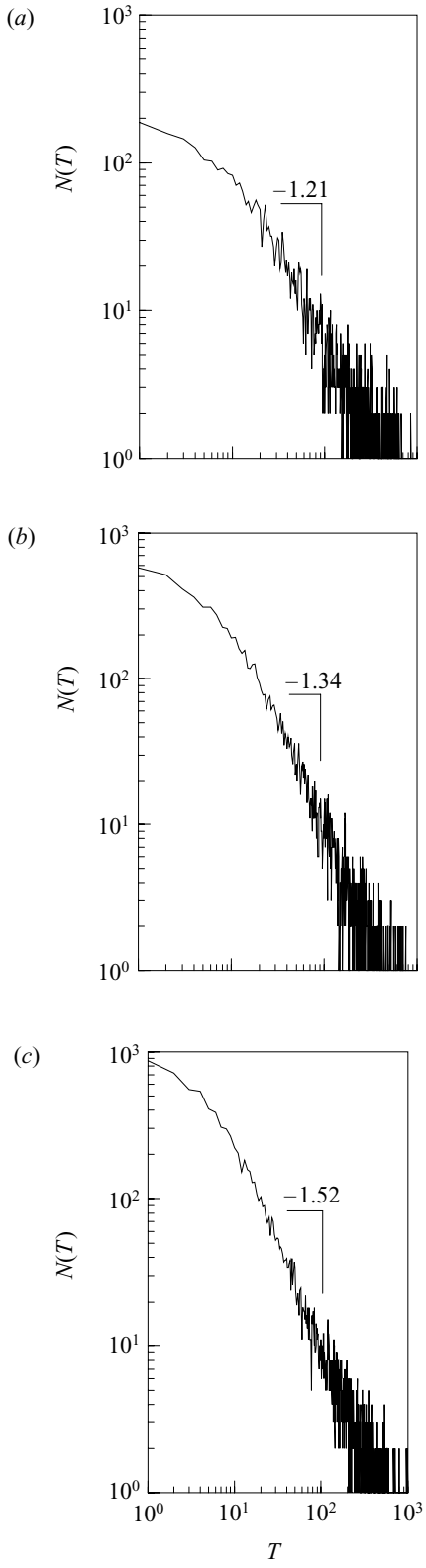

Figure 5. Lifetime distribution for a long time average of three different realizations of model B in the steady-state regime ($N = 4000$, $S = 200$, $\mu = 0.005$ and $c_i = e_i = 0.01$ for all species, with (*a*) $C = 0.1$; (*b*) $C = 0.3$; and (*c*) $C = 0.5$). The observed slopes are indicated. For small interactin rates we obtain $\theta \approx 1$ and as C increases, values close to $\theta \approx 3/2$ are observed. Using breeding bird populations in the USA, Keitt & Stanley (1998) found a value of 1.61.

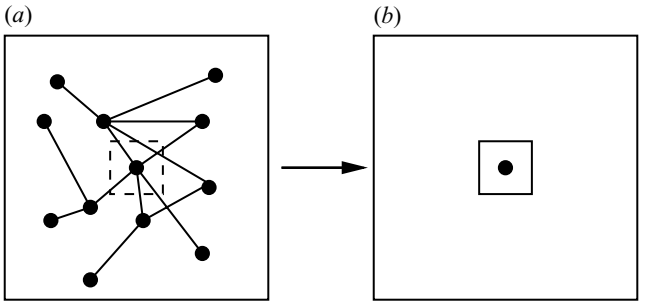

Figure 6. Mean field approximation applied to the multispecies food web model. The real web (*a*) is replaced by a mean-field system (*b*), where a given species (central square) 'sees' the rest of the ecosystem as a homogeneous system.

sition rates, i.e. the probability per unit time that, being at n, a jump occurs to $n - 1$ or to $n + 1$, respectively.

Two different processes will contribute to each transition rate in our model: those linked with internal interactions through Ω and those due to immigration. As an example, let us consider r_n. Assuming a population of N individuals, S species and a matrix connectivity C_π, r_n will be decomposed into two terms:

$$r_n \equiv W(n-1|n) = W_\Omega(n-1|n) + W_\mu(n-1|n), \tag{4.2}$$

where W_Ω and W_μ indicate interaction and immigration-dependent transitions, respectively. It is not difficult to show that

$$W_\mu(n-1|n) = \mu\left(1 - \frac{1}{S}\right)\frac{n}{N} \tag{4.3}$$

$$W_\Omega(n-1|n) = [1 - (1 - C_\pi)^2](1 - \mu)\frac{n}{N}\left(\frac{N-n}{N-1}\right). \tag{4.4}$$

The first of them is easily understandable: we choose one individual from the species considered (with probability n/N) and replace it by another individual belonging to a different species (with probability μ). In order to guarantee that it belongs to some *other* species, the factor $1 - 1/S$ is used.

The second term can also be derived from simple arguments. In this case, we take, with probability $1 - \mu$, two individuals from the system, one from our species and another from a different species. If they interact (with probability C^*) then one of them wins, as defined by our rules (two possible pairs are available and the probability that the second wins over the first is just one half). The probability C^* is given by

$$C^* = 1 - (1 - C_\pi)^2, \tag{4.5}$$

which is easily understandable: since the elements of Ω are chosen at random, the probability of no interaction is $P[\Omega_{ij} = \Omega_{ji} = 0] = (1 - C_\pi)^2$ and interaction will otherwise occur. The final one-step transition rates are given by

$$r_n = C^*(1 - \mu)\frac{n}{N}\frac{N-n}{N-1} + \frac{\mu}{S}(S-1)\frac{n}{N} \tag{4.6}$$

$$g_n = C^*(1 - \mu)\frac{n}{N}\frac{N-n}{N-1} + \frac{\mu}{S}\left(1 - \frac{n}{N}\right). \tag{4.7}$$

These one-step processes occur whenever the stochastic dynamics consists of the birth and death of individuals. The name does not imply that it is not possible for n to jump by two or more units in a time Δt, but only that the probability for this to happen is $\mathcal{O}(\Delta t^2)$, and therefore negligible for small Δt. The previous transition probabilities are completed by the natural boundary conditions of minimum zero population and maximum N population (i.e. we have $r_0 = 0$ (and can define $g_{-1} = 0$) and $g_N = 0$ (and define $r_{N+1} = 0$)).

Using standard methods from the theory of stochastic processes (van Kampen 1981) it can be shown that the stationary distribution reads:

$$P_s(n) = \frac{g_{n-1}g_{n-2}\ldots g_0}{r_n r_{n-1}\ldots r_1} P_s(0);\ n = 1,\ldots,N. \tag{4.8}$$

The constant $P_s(0)$ can be determined from the normalization condition given by

$$\sum_{n=0}^{N} P_s(n) = P_s(0) + \sum_{n>0} P_s(n) = 1: \tag{4.9}$$

$$(P_s(0))^{-1} = 1 + \sum_{n=1}^{N} \frac{g_{n-1}g_{n-2}\cdots g_0}{r_n r_{n-1}\cdots r_1}. \tag{4.10}$$

It can be shown, after some algebra, that

$$\begin{aligned}(P_s((0)))^{-1} &= \sum_{n=0}^{N} \binom{N}{n} \frac{\Gamma(n+\lambda^*)}{\Gamma(\lambda^*)} \frac{\Gamma(\nu^* - n)}{\Gamma(\nu^*)} \\ &= \sum_{n=0}^{N} \binom{N}{n} (-1)^n \frac{\Gamma(n+\lambda^*)}{\Gamma(\lambda^*)} \frac{\Gamma(1-\nu^*)}{\Gamma(n+1-\nu^*)}.\end{aligned} \tag{4.11}$$

This sum takes the form of a Jacobi polynomial $P_N^{(\alpha,\beta)}(x)$ (Abramowitz & Stegun 1965) with $\alpha = -\nu^*$, $\beta = \lambda^* + \nu^* - (N+1)$ and $x = -1$, which can itself be expressed in terms of gamma functions ($\Gamma(x)$) for this value of x. Therefore, using equation (4.8) we find

$$P_s(n) = \binom{N}{n} \frac{\Gamma(n+\lambda^*)}{\Gamma(\lambda^*)} \frac{\Gamma(\nu^* - n)}{\Gamma(\nu^* - N)} \frac{\Gamma(\lambda^* + \nu^* - N)}{\Gamma(\lambda^* + \nu^*)}, \tag{4.12}$$

where the following notation has been used:

$$\begin{aligned}&\mu^* = \mu/[(1-\mu)SC^*], \lambda^* = \mu^*(NH - 1) \\ &\quad \text{and} \quad \nu^* = N + \mu^*(N-1)(S-1).\end{aligned} \tag{4.13}$$

When $N > S \gg 1$, $N \gg 1$ and $N \gg n > 0$ (i.e. small characteristic population values) and assuming in addition that μ is small, we find (McKane *et al.* 2000; Solé *et al.* 2000):

$$P_s(n) = \frac{\mathcal{K}}{n} \exp\left(\frac{-\mu}{C^*(1-\mu)} n\right), \tag{4.14}$$

where the normalization constant is given by

$$\mathcal{K} = \lambda^* \left(\frac{\mu}{(1-\mu)C^*}\right)^{\lambda^*}. \tag{4.15}$$

In figure 7, using simulations both in model A and B for different immigration rates, we can see that, as the immigration rate is reduced (and thus interactions dominate in the dynamics) the distributions display long tails. Together with the (non-realistic) Gaussian distribution, we find the familiar lognormal and power-law shapes. As we can see in inset plots, the scaling exponent for the power law agrees both with the mean field prediction ($\gamma = 1$) and empirical data (figure 2). In fact, the mean field model has been shown to provide Gaussian and lognormal distributions for different parameter ranges (McKane *et al.* 2000). For very high immigration rates or very low connectivity values, the system is dominated by the arrival of external immigrants, and species evolve randomly without interacting with each other. In these regimes Gaussian distributions are observed. For intermediate values of immigration and connectivity values the populations are dominated neither by external inputs nor by internal dynamics, and lognormal distributions are observed. Finally, for very low immigration values and high connectivity values, the system is dominated by internal dynamics, and power-law distributions are observed (table 1).

(c) *Species–connectivity relation*

The second statistical feature that can be derived from our analysis is the well-known scaling in the species–connectivity relation. Our model confirms the conjecture that, as the number of species reaches a given critical value (for each given connectivity) then no further increase in species number is possible. Species interact with an average of *ca.* $C\langle S\rangle$ species and a constant turnover is observable. If we artificially increase the diversity by dropping additional species into the system, a rapid decrease in $\langle S\rangle$ is observed until the critical number is recovered.

In this context, a qualitative argument can be provided in order to illustrate this result. Let us consider a deterministic mean field approach, where species interact through a predefined matrix. Let S be the maximum allowed number of species. The deterministic counterpart of our model would read:

$$\frac{\mathrm{d}s(t)}{\mathrm{d}t} = \mu\left(1 - \frac{s(t)}{S}\right) - c(t)s(t), \tag{4.16}$$

$$\frac{\mathrm{d}c(t)}{\mathrm{d}t} = s(t)(C_\pi - c(t)). \tag{4.17}$$

These equations can be understood as follows. The two terms on the right-hand side of equation (4.16) represent the rate of change of species due to external immigration and due to internal interaction. The first of these terms, that due to external interaction, can, as a preliminary step, be explained by considering the case $S \to \infty$. If the species pool were infinitely large, every new immigrant individual would belong to a new species and $s(t)$ would increase by one in time μ^{-1}. To correct this rate of increase for the fact that S is finite, but still large, a linear decrease of the form $[1 - (s(t)/S)]$ has been assumed. The second term, that due to internal interaction, is negative since any internal interaction provides a chance for the number of species in the system to decrease. It is proportional to the probability of an internal interaction, $c(t)$, and to the number of species present $s(t)$. The second equation may be understood by imagining that the probability of interaction is very small. Thus, the number of species and the probability of interaction will increase, since more species means more opportunities to interact. However, if the probability of interaction is large, the number of species and the probability of interaction will start to decrease.

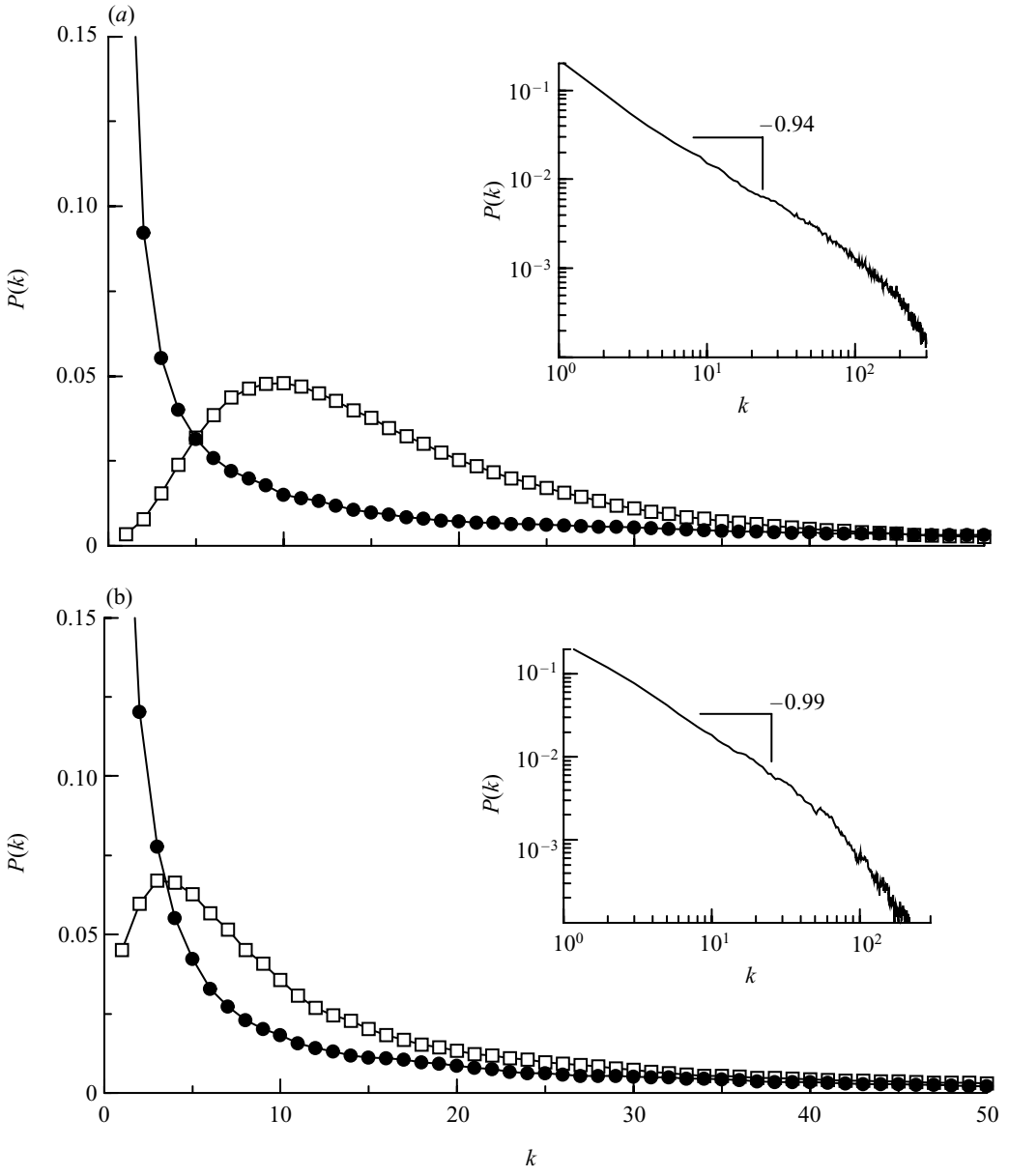

Figure 7. Species–abundance distributions obtained from (*a*) model A and (*b*) model B. As the immigration rate decreases, long-tailed distributions become more common. Here we show the lognormal distribution (open squares) and power laws (filled circles). Both have been obtained using $S = 200$, $N = 4000$ and immigration rates of $\mu = 0.05$ (lognormal) and $\mu = 0.005$ (scale-free distribution). For model B, the death and colonization rates are set at $e = 0.01$ and $c = 0.01$ respectively, for all species. The insets show a log–log plot of the power-law solutions. We can see that the exponents are consistent with field data (i.e. $\gamma \approx 1$).

Table 1. Comparison between field data and the stochastic model A.
(Model B and the spatially explicit model give similar statistics. HF: highly fluctuating. In the lifetime relationship, the lower bound of the exponent is provided by Keitt & Marquet (1996).)

property	field data	model
species–connectivity	$S \approx kC^{-1+\epsilon}$, $0 \leqslant \epsilon \leqslant 0.5$	$S = kC^{-1+\epsilon(\mu)}$
scaling in diversity	$P(n) \propto n^{-\gamma}$, $\gamma \approx 1$	$P(n) \propto n^{-\gamma}$, $\gamma \approx 1$
lifetimes	$N(T) \approx T^{-\theta}$; $\leqslant 1 \leqslant \theta \approx 1.6$	$N(T) \approx T^{-\theta}$; $(1 < \theta < 3/2)$
population dynamics	HF, $(\lambda_L \approx 0)$	HF, marginal
Gaussian distribution	not observed	$C \rightarrow 0$, $\mu \rightarrow 1/2$
lognormal distribution	common	$C \rightarrow 0.5$, $\mu \approx 0.1$
power-law distribution	observed	$C \rightarrow 1$, $\mu \rightarrow 0$
SARs	$S \propto A^z$, $0 < z < 1$	$S \propto A^z$, $0 < z < 1$

These considerations lead to equation (4.17), where C_π is the equilibrium value of $c(t)$. Two general observations may be made which follow directly from equations (4.16) and (4.17). (i) If no interactions were allowed to occur (assuming a large number of individuals), then the number of species reaches a maximum value of S. (ii) If the system evolves from small values of $c(t)$, then it increases with the number of species until it reaches the value C_π, imposed by the connectivity matrix. This limits the growth rate of the number of species. In other words, interactions inhibit further increase of diversity.

The model defined by equations (4.16) and (4.17) has a single steady state:

$$(s^*,c^*) = \left(\frac{\mu S}{C_\pi S + \mu}, C_\pi\right). \tag{4.18}$$

In fact, we can see that the steady state associated with the number of species follows a hyperbolic relation with C_π for large S and small immigration rates:

$$s^* \rightarrow \frac{\mu}{C_\pi}. \tag{4.19}$$

It is interesting to note that our argument is not based in linear stability arguments but on the presence of a positive feedback from diversity to connectivity plus a reverse, negative feedback in the other direction. This is in fact a globally stable attractor. The Jacobi matrix for this system is given by

$$\boldsymbol{L} = \begin{pmatrix} \partial\dot{s}/\partial s & \partial\dot{s}/\partial c \\ \partial\dot{c}/\partial s & \partial\dot{c}/\partial c \end{pmatrix}. \tag{4.20}$$

At the fixed point, we have

$$\boldsymbol{L}(s^*,c^*) = \begin{pmatrix} -\mu/S - C_\pi & -s^* \\ 0 & -s^* \end{pmatrix}, \tag{4.21}$$

which trivially gives the two negative eigenvalues: $\lambda_1 = -\mu/S - C_\pi$ and $\lambda_2 = -s^*$. Conversely, it is easy to show that, if the initial connectivity is already C_π (i.e. the initial number of species already interact with a connectivity C), then the first equation allows us to solve for the mean-field temporal evolution of $s(t)$, assuming that no species were present at $t = 0$. This so-called colonization curve (MacArthur & Wilson 1967) is given by

$$s(t) = \frac{\mu}{\Omega}(1 - \mathrm{e}^{-\xi t}), \tag{4.22}$$

where $\xi \equiv \mu/S + C_\pi$ gives the speed at which the steady state is reached. It is significant that the final result is similar to that derived from classic island biogeography theory (MacArthur & Wilson 1967). Specifically, MacArthur & Wilson's derivation of the colonization curve was obtained by integrating the difference between the time-curves of the immigration I, and extinction E, rates, i.e.

$$s(t) = \int_0^t (I(t) - E(t))\mathrm{d}t.$$

A more controlled derivation of the actual scaling relation can be obtained from the stochastic model (McKane *et al.* 2000). As the number of species can be written as $\langle S\rangle = (1 - P_s(0))S$ and it can be shown that $P_s(0) = (\mu^* S)^{\mu^* N}$, for the range of parameters considered in the derivation of the power law solution of equation (4.8), it gives $\langle S\rangle = S\mu^* N \ln(1/(\mu^* S))$. Substituting in the expression for μ^* gives

$$\langle S\rangle = \frac{\mu N}{(1-\mu)C^*}\left[\ln\left(\frac{1-\mu}{\mu}\right) = \ln C^*\right] \approx \mathscr{A}(C^*)^{-1+\epsilon(\mu)}, \tag{4.23}$$

where ϵ is given by

$$\epsilon^{-1} = \ln\left(\frac{1-\mu}{\mu}\right) \approx \ln\frac{1}{\mu} \tag{4.24}$$

and $\mathscr{A}$ is a constant given by

$$\mathscr{A} = N\epsilon^{-1}\exp(-\epsilon^{-1}). \tag{4.25}$$

The additional conditions under which equation (4.23) holds are $\lambda^* \ll \epsilon$ and $|\ln C^*| \ll |\ln\mu|$, where $\lambda^* = \mu(N-1)/[(1-\mu)SC^*]$.

In figure 8 we illustrate the simulated values for the species–connectivity relation for two different immigration rates. The log–log plot allows the presence of a scaling relation to be appreciated, with a changing exponent that depends on μ, as expected.

5. SPATIALLY EXTENDED SYSTEMS

A further test of the generality of our model is provided by the consideration of explicit spatial degrees of freedom (Bascompte & Solé 1995, 1998; Durrett 1999). The most important relation that can be investigated as a result of this extension of the model is the relation between species richness and the area covered by the ecosystem under consideration.

SARs have been observed for a long time and are considered to be one of the few genuine laws of community ecology. The standard (but not unique) form of this relation is a power-law relation:

$$S = \alpha A^z, \tag{5.1}$$

where α is a constant and S is the total number of species observed within a given area A. The exponent of this scaling relation, z, takes a range of values between zero and one depending on a number of features. Within a biogeographic region it takes typical values of 0.1–0.2. Considering islands of different area, the z exponent takes higher values (0.25–0.45), and comparing the whole biotas of different biogeographic regions, the exponent takes the highest values (0.9) (Rosenzweig 1995). The SAR has been used in many applications and is particularly relevant for characterization of community structure, estimation of species richness, and estimation of species loss rates through habitat destruction, or to determine reserve sizes.

To extend the previous model into space is relatively easy. Both models A and B admit natural spatial extensions. Let us construct the spatially explicit counterpart to model A. The previous rules have now to be extended to a lattice of sites that are occupied by individuals of different species. $S_{ij} \in \Sigma$ represents the species present at the (i,j)th site (here $1 < i, j < L$). Our rules now read:

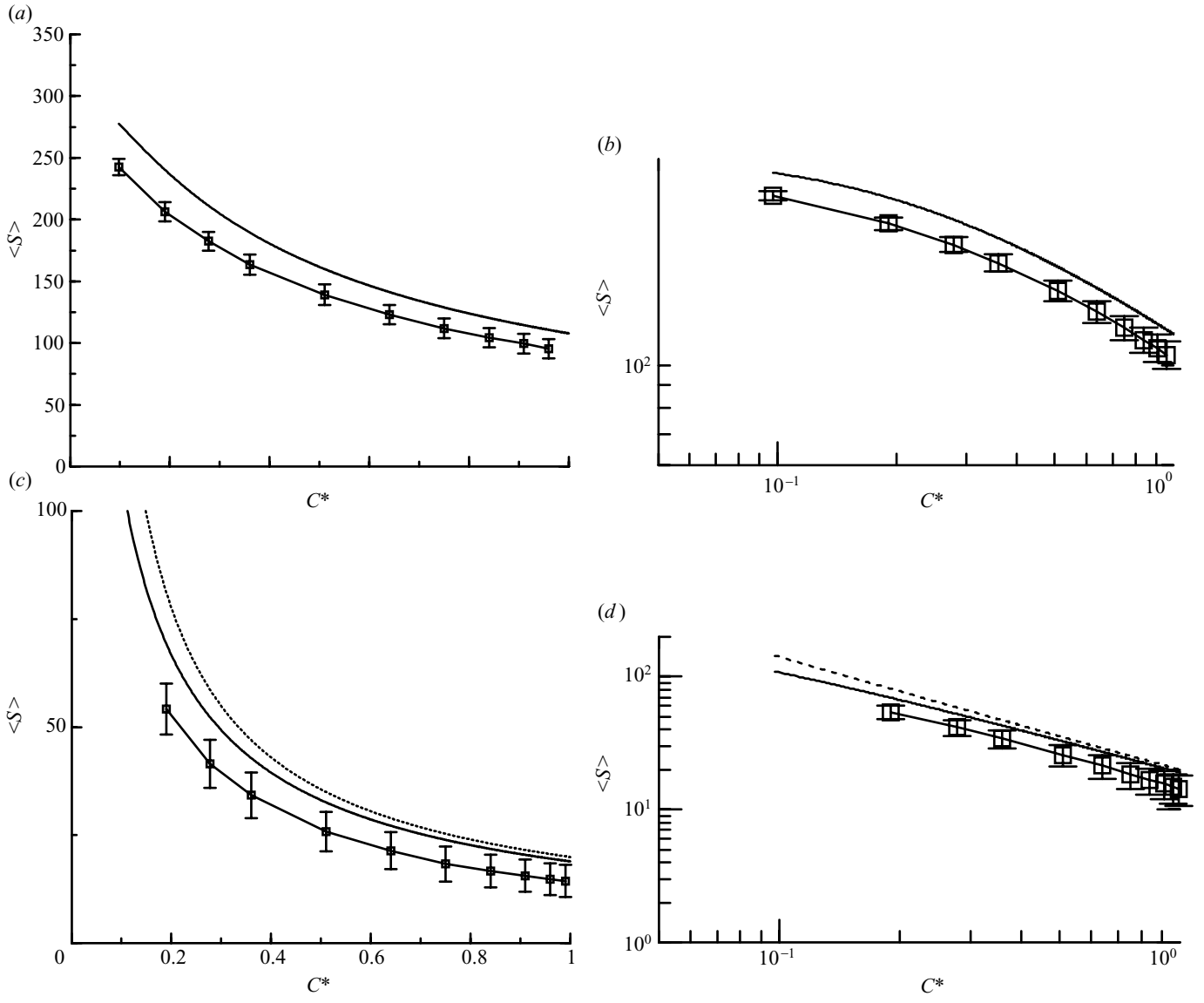

Figure 8. Species–connectivity relationship. Two simulations are presented for two immigration values. Plots (*a*) and (*b*) correspond to a simulation with a higher value corresponding to plots (*c*) and (*d*). Although the mean field approach overestimates systematically the average number of species at steady state, the qualitative hyperbolic behaviour of $S-C$ curves is well captured. Standard deviations from the ensemble average value are also shown. In (*a*) and (*b*), the conditions required for the approximation given by equation (4.23) to be valid are not fulfilled. Apart from the simulated values, in this case the other plotted curve is the exact mean field relation $\langle S\rangle = (1 - P_s(0))S$. In contrast, in (*c*) and (*d*), the conditions needed to apply equation (4.23) are quite well fulfilled and two other curves are plotted: the exact mean field relation (solid line) and the approximation (dotted line).

(i) Immigration: a randomly chosen site occupied by species S_{ij} is replaced by a species randomly chosen from the species pool, i.e. $S'_{ij} \in \Sigma(S)$:

$$S_{ij} \xrightarrow{\mu} S'_{ij}, \tag{5.2}$$

with a probability μ—the same value for all species.

(ii) Interaction: given a randomly chosen site occupied by a species $S_{ij} \in \Sigma$ we select one of its q nearest neighbours (here we take $q = 8$), say $S_{rs} \in \Sigma$, and perform the replacement $S_{ij} = S_{rs}$ if the interaction matrix allows it (as defined in the non-spatial counterpart).

Because the rules of interaction are now local (immigration introduces non-local effects required in order to maintain a stable diversity), we should expect to observe spatial clusters of sites occupied by the same species. An example of the obtained patterns is shown in figure 9. In order to define a colour scale, we have used a dominance index η_i for each species, defined from the interaction matrix as follows:

$$\eta_i = \frac{1}{S}\sum_{j=1}^{S} \theta[\Omega_{ij} - \Omega_{ji}], \tag{5.3}$$

where $\theta[x] = 1$ when $x > 0$ and zero otherwise. Here $\eta_i \in [0,1]$ indicates how probable it is that a species i will invade (on average) a nearest-neighbour site occupied by another species from Σ.

In both models, small immigration or larger C favour the formation of larger connected patches of the same type. As immigration or interaction rates increase (allowing an easier invasion of patches) patch size

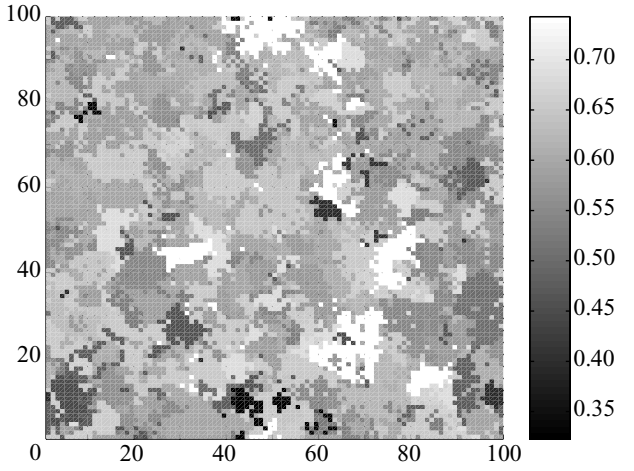

Figure 9. Spatial snapshot generated by the stochastic model on a 100×100 lattice for a system involving $S = 150$ species and $C = 0.2$, $\mu = 0.005$. The grey scale has been generated by using a parameter—the dominance index parameter of equation (5.3)—that measures the colonization ability of each species.

becomes smaller and species are more randomly scattered through the lattice. This is reflected in the SARs, as shown in figure 10. We can see that the exponent z increases with μ (model A) since higher immigration makes it easier to find any species during the sampling. Conversely, as C becomes smaller, and patches shrink in size, saturation occurs more rapidly and larger z values are also observed. The range of values obtained is consistent with field observations from rainforest plots (Condit *et al.* 1996; Plotkin *et al.* 2000).

In summary, in table 1 the field data and model results are compared with regard to the different well-established regularities observed in natural systems that have been addressed. A species–connectivity relationship is predicted by model A at low immigration regimes. Highly fluctuating populations showing complex dynamics including chaos, and scaling relations for species lifetime distributions characterize temporal dynamics. The model in different immigration regimes also recovers the different shapes of abundance distribution curves. Finally, the behaviour of the exponent z of the SAR is well captured by the modelling approach presented: the exponent decreases when the relative importance of interactions within the system increases with respect to external immigration events, in agreement with earlier theoretical studies (Durrett & Levin 1996).

6. DISCUSSION

We have further explored a previously presented stochastic model of multispecies communities. The aim of our study was to analyse the robustness of our previous findings, to extend them into a spatially explicit context and to propose a new unifying framework able to include a disparate number of features reported from complex ecologies. The present results can be summarized as follows.

(i) Our stochastic models display complex time fluctuations, which can exhibit deterministic features under low-diversity (S) and high-connectivity (C) conditions. A general trend is the presence of more complex and variable time-series as immigration allows the simultaneous coexistence of many species.

(ii) The species–abundance distributions obtained from both models are able to reproduce the long-tailed shapes characteristic of real ecologies. In particular, for small immigration rates and not very small connectivities, power-law and lognormal distributions are obtained, in agreement with field data. The dynamics of these distributions is also in agreement with the patterns of species–rank distributions exhibited by ecological succession.

(iii) The connectance and species diversity displayed by the stationary states in both models are linked to the observed scaling law $S \propto C^{-1+\epsilon}$, with ϵ dependent upon immigration rates. This result and mean field calculations indicate that the deviations from the hyperbolic law $S \propto C^{-1}$ are due to the fluctuations arising from the presence of immigration.

(iv) The spatially extended counterparts of our models, including limited dispersal and competition, leads to a SAR $S = \alpha A^z$ consistent with observed patterns in rainforest plots. The exponent z increases with larger immigration rates and decreases as the connectivity increases. Therefore, in general, the exponent z is greater the greater the relative importance of immigration processes are with respect to internal dynamics.

The driving force in ecology is the increase in diversity due to either immigration or speciation: assuming a given average C, as the number of species increases the system interactions increase too, and competition and other forces counterbalance the driving by triggering extinction events as the interactions among components increase (figure 11). The system is naturally poised at the critical boundary. This observation would suggest that ecological systems are self-organized critical. However, real ecosystems (as happens to be the case with other complex systems) lack some of the ingredients required in order to define them as self-organized critical. First, they are, in many cases, influenced by external perturbations of a different nature and cannot simply be considered as purely driven by internal dynamics. Second, interactions happen to occur in a non-homogeneous way (different species interact with different strengths) and thus the local rules of interaction might be very different from place to place. Third, although the increase in diversity is a driving force that pushes ecosystems towards the instability boundary, such driving does not need to be very slow (which seems to be a strong condition for SOC dynamics) and thus the system does not necessarily have time to relax before a new species enters the system. The last point makes it possible to observe long-tailed distributions having some characteristic maximum, as happens with the lognormal shapes.

Here we propose a new concept, *self-organized instability*, as a unifying framework able to include the range of patterns observed in ecological systems and provide a complete view of the previous properties within a single theoretical approximation. Under the constant immigration of species, diversity increases until a critical num-

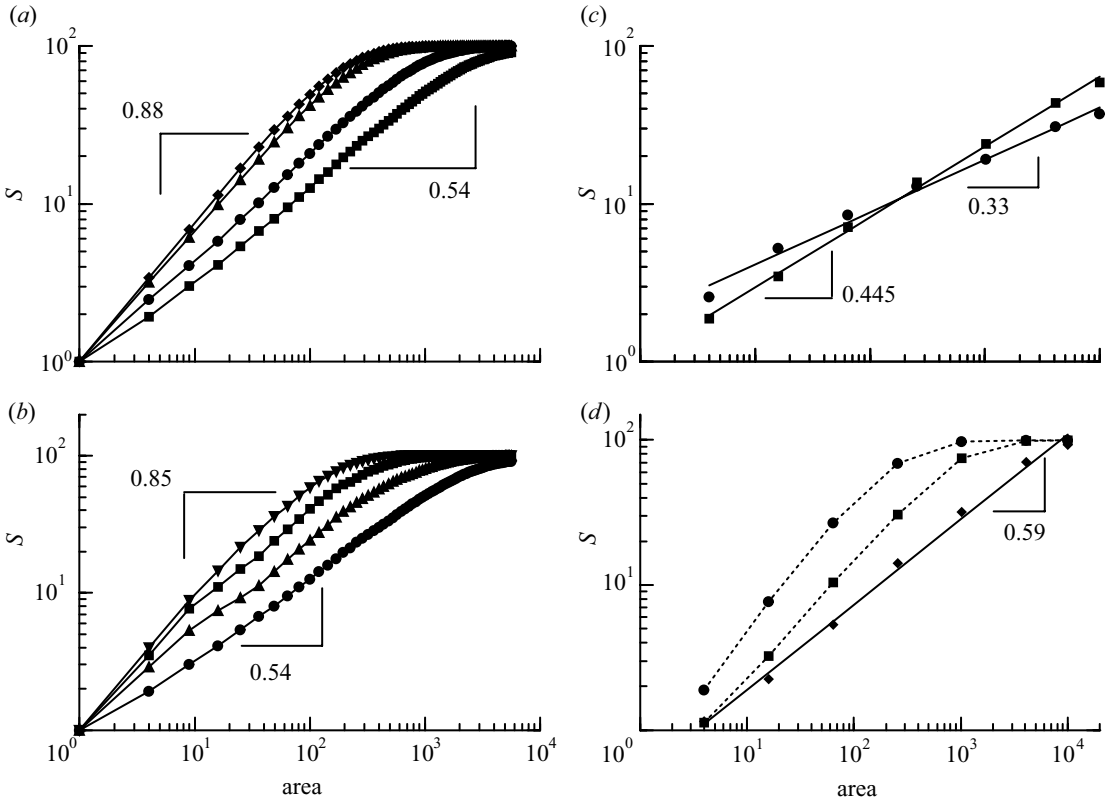

Figure 10. Comparison of the multispecies lattice (*a*,*b*) model A and (*c*,*d*) model B with regard to the relation between diversity (number of species, *S*) and SAR. Each individual can interact with a randomly elected individual from its eight nearest neighbours. For the low-immigration regimes, the power-law behaviour in the SAR ($S \propto A^z$) holds for larger areas. In both models, the slope of the SAR decreases as the relative importance of immigration events diminishes with respect to internal dynamics, in agreement with the results already observed in similar multispecies lattice models (Durrett & Levin 1996). In all simulations a 100×100 lattice was used, and 5×10^6 elementary updating steps were performed, with only the last 5×10^5 being used to perform averages. In model B, a default value of $C = 0.5$ was used. The same extinction and immigration values for all species, were used in all simulations. (*a*) $C = 0.5$; squares, $\mu = 0.001$; circles, $\mu = 0.005$; diamonds, $\mu = 0.1$; triangles $\mu = 0.01$. (*b*) $\mu = 0.001$; up triangles, $C = 0.1$; circles, $C = 0.2$; squares, $C = 0.05$; down triangles, $C = 0.01$. (*c*) $\mu = 0.001$; squares, $e = 0.05$; circles, $e = 0.005$. (*d*) $e = 0.5$; circles, $\mu = 0.5$; squares, $\mu = 0.05$; diamonds, $\mu = 0.005$.

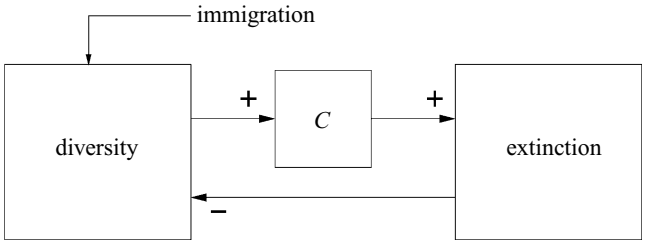

Figure 11. Feedback loops leading to instability. For an ecosystem, the constant addition of new species by immigration increases the likelihood of interactions. Such interactions limit diversity and trigger extinctions, thus inhibiting further increases of diversity.

ber of resident species is reached. Now instability acts as a barrier preventing further increases in diversity (although species turnover is observed). The dynamical, structural and statistical features of the simulated ecosystems result from a single, basic mechanism of community organization.

How different are the causal explanations presented from those operating in natural systems? The simple models that we have considered are, of course, oversimplifications of reality. They do not include, as happens with most other ecological models, most of the details that define species and their relationships between them and the environment. No external fluctuations, physiology, energetics or trade-offs are explicitly present. However, despite these drawbacks, the power of our approximation seems clear. Why is that? We can conjecture that nonlinear dynamics and the dynamical features that emerge as a consequence of stochastic dynamics and marginal stability are much more important than thermodynamic considerations (at least at the scales considered). This view is not new in ecology: the constraints operating in food chain lengths are a clear example (Morin (1999) and references cited therein). Although thermodynamic arguments suggest that longer chains will be observed at higher productivities, in fact threshold instabilities arising from nonlinear dynamics lead to shorter chains.

Perhaps this underlies the success of community models based on dynamical systems approaches. In these models, instability is ultimately responsible for the observed fluctuations and these allow the macroscopic laws observable in real ecosystems to be obtained. We do not know if our approach can be translated into a broad range of situations, but it provides a well-defined mechanism that suggests that our biosphere can have predictable properties arising from complex fluctuations. There is indeed pre-

dictability here: the overall features present in our models correspond to observable regularities that indicate that global patterns are actually 'attractors' of the dynamics. In this sense, we can see that some kind of equilibrium state can be defined at the community level. The changes in species composition, the fluctuations of their populations as well as the presence of rarity are, however, the fingerprint of the underlying instability. Under our approximation, ecological complexity results from the conflict between the tendency to higher diversity and the negative feedbacks arising from interactions. Future studies including evolutionary responses might help to understand the evolutionary consequences of these dynamical patterns.

We thank Javier Gamarra and Jose Montoya for useful discussions. This work has been supported by a grant PB97-0693 and by the Santa Fe Institute (R.V.S.), by a CIRIT grant 1999FI 00524 UPC APMARN (D.A.) and by EPSRC grant GR/K79307, NSF grant DMR-99-70690 and the British Council (A.M.).

REFERENCES

Abramowitz, M. & Stegun, I. A. (eds) 1965 *Handbook of mathematical functions*. New York: Dover Publications.

Alonso, D. & Solé, R. V. 2000 The DivGame simulator: a stochastic cellular automata model of rain-forest dynamics. *Ecol. Model.* **133**, 131–141.

Amaral, L. A. N., Buldyrev, S., Havlin, S., Salinger, M. A. & Stanley, H. E. 1998 Power law scaling for a system of interacting units with complex internal structure. *Phys. Rev. Lett.* **80**, 1385–1388.

Ariño, A. & Pimm, S. L. 1995 On the nature of population extremes. *Evol. Ecol.* **9**, 429–443.

Bak, P., Tang, C. & Wiesenfeld, K. 1987 Self-organized criticality: an explanation for 1/*f* noise. *Phys. Rev. Lett.* **59**, 381–384.

Bak, P., Chen, K. & Tang, C. 1990 The forest fire model and some thoughts on turbulence. *Phys. Lett.* A **147**, 297–300.

Bascompte, J. & Solé, R. V. 1995 Rethinking complexity—modelling spatiotemporal dynamics in ecology. *Trends Ecol. Evol.* **10**, 361–366.

Bascompte, J. & Solé, R. V. (eds) 1998 *Modelling spatiotemporal dynamics in ecology*. Berlin: Springer.

Bazzaz, F. A. 1975 Plant species diversity in oldfield successional ecosystems in southern Illinois. *Ecology* **56**, 485–488.

Bell, G. 2000 The distribution of abundance in neutral communities. *Am. Nat.* **155**, 606–616.

Bell, G. 2001 Neutral macroecology. *Science* **293**, 2413–2418.

Binney, J. J., Dowrick, N. W., Fisher, A. J. & Newman, M. E. J. 1993 *The theory of critical phenomena*. Oxford: Clarendon Press.

Brown, J. H. 1995 *Macroecology*. University of Chicago Press.

Camacho, J. & Solé, R. V. 2000 Scaling in ecological size spectra. Santa Fe Institute working paper 99-12-076.

Condit, R., Hubbell, S. P., LaFrankie, J. V., Sukumar, R., Manokaran, N., Foster, R. B. & Ashton, P. S. 1996 Species–area and species–individual relationships for tropical trees: a comparison of three 50-ha plots. *J. Ecol.* **84**, 549–562.

Drake, J. A. 1990*a* The mechanics of community assembly and succession. *J. Theor. Biol.* **147**, 213–233.

Drake, J. A. 1990*b* Communities as assembled structures: do rules govern pattern? *Trends Ecol. Evol.* **5**, 159–163.

Drossel, B. & Schwabl, F. 1992 Self-organized critical forest fire model. *Phys. Rev. Lett.* **69**, 1629–1632.

Durrett, R. 1999 Stochastic spatial models. *Soc. Ind. Appl. Meth. Rev.* **41**, 677–718.

Durrett, R. & Levin, S. A. 1994 Stochastic spatial models: a user's guide to ecological applications. *Phil. Trans. R. Soc. Lond.* B **343**, 329–350.

Durrett, R. & Levin, S. A. 1996 Spatial models for species–area curves. *J. Theor. Biol.* **179**, 119–127.

Ellner, S. 1988 Estimating attractor dimensions from a limited data: a new method with error estimates. *Phys. Lett.* A **133**, 128–131.

Ellner, S. & Turchin, P. 1995 Chaos in a noisy world—new methods and evidence from time series analysis. *Am. Nat.* **145**, 343–375.

Elton, C. S. 1958 *Ecology of invasions by animals and plants*. London: Chapman & Hall.

Gamarra, J. G. P. & Solé, R. V. 2000 Bifurcations and chaos in ecology: lynx returns revisited. *Ecol. Lett.* **3**, 114–121.

Hastings, A., Hom, C., Ellner, S., Turchin, P. & Godfray, H. 1993 Chaos in ecology: is mother nature a strange attractor? *A. Rev. Ecol. Syst.* **24**, 1–33.

Hogg, T., Huberman, B. & McGlade, J. M. 1989 The stability of ecosystems. *Proc. R. Soc. Lond.* B **237**, 43–51.

Hubbell, S. 1979 Tree dispersal, abundance and diversity in a tropical dry forest. *Science* **203**, 1229–1309.

Hubbell, S. 2001 *The unified neutral theory of biodiversity and biogeography*, Monographs in population biology. Princeton University Press.

Jensen, H. J. 1998 *Self-organized criticality*. Cambridge University Press.

Keitt, T. & Marquet, P. 1996 The introduced Hawaiian avifauna reconsidered: evidence for self-organized criticality? *J. Theor. Biol.* **182**, 161–167.

Keitt, T. & Stanley, H. E. 1998 Dynamics of North American breeding bird populations. *Nature* **393**, 257–260.

Leakey, R. & Lewin, R. 1996 *The sixth extinction*. New York: Doubleday.

Levin, S. A. 1998 Ecosystems and the biosphere as complex adaptive systems. *Ecosystems* **1**, 431–436.

Levin, S. A. 1999 *Fragile dominion*. Reading, MA: Perseus Books.

MacArthur, R. H. & Wilson, E. O. 1967 *The theory of island biogeography*. Princeton University Press.

McCann, K., Hastings, A. & Huxel, G. R. 1998 Weak trophic interactions and the balance of nature. *Nature* **395**, 794–797.

McCann, K. S. 2000 The diversity–stability debate. *Nature* **405**, 228–233.

McKane, A., Alonso, D. & Sol, R. V. 2000 A mean field stochastic theory for species-rich assembled communities. *Phys. Rev* E **62**, 8466–8484.

Malamud, B. D., Morein, G. & Turcotte, D. L. 1998 Forest fires: an example of self-organized critical behavior. *Science* **281**, 1840–1842.

Margalef, R. 1994 Through the looking glass: how the marine phytoplankton appears through the microscope when graded by size and taxonomically sorted. *Sci. Marina* **58**, 87–101.

Martinez, N. D. 1992 Constant connectance in community food webs. *Am. Nat.* **139**, 1208–1218.

Martinez, N. D. 1994 Scale-dependent constraints in food web structure. *Am. Nat.* **144**, 935–953.

Marro, J. & Dickman, R. 1999 *Nonequilibrium phase transitions in lattice models*. Cambridge University Press.

Maurer, B. A. 1999 *Untangling ecological complexity*. University of Chicago Press.

May, R. M. 1972 Will a complex system be stable? *Nature* **238**, 413.

May, R. M. 1974 *Stability and complexity in model ecosystems*, 2nd edn. Princeton University Press.

May, R. M. 1975 Patterns of species abundance and diversity. In *Ecology and evolution of communities* (ed. M. L. Cody & J.

M. Diamond), pp. 81–118. Cambridge, MA: Harvard University Press.
Montoya, J. M. & Solé, R. V. 2002*a* Small world patterns in food webs. *J. Theor. Biol.* **214**, 405–412.
Montoya, J. M. & Solé, R. V. 2002*b* Topological properties of food webs: from real data to ecological assembly models. *Oikos* (Submitted.)
Morin, P. J. 1999 *Community ecology*. Boston, MA: Blackwell Science.
Odum, E. P. 1953 *Fundamentals of ecology*. Philadelphia, PA: Saunders.
Pachepsky, E., Crawford, J. W., Brown, J. L. & Squire, G. 2001 Towards a general theory of biodiversity. *Nature* **410**, 923–926.
Paine, R. T. 1966 Food web complexity and species diversity. *Am. Nat.* **100**, 65–75.
Pielou, E. C. 1969 *An introduction to mathematical ecology*. New York: Wiley.
Pimm, S. 1982 *Food webs*. London: Chapman & Hall.
Pimm, S. 1991 *The balance of nature*. University of Chicago Press.
Polis, G. A. 1991 Complex trophic interactions in deserts: an empirical critique of food-web theory. *Am. Nat.* **138**, 123–155.
Plotkin, J. B. (and 13 others) 2000 Predicting species diversity in tropical forests. *Proc. Natl Acad. Sci. USA* **97**, 10 850–10 854.
Pueyo, S. 2002 A theory of ecological diversity. *Diversity Scaling* (Submitted.)
Reagan, D. & Waide, R. (eds) 1996 *The food web of a tropical rainforest*. University of Chicago Press.
Renshaw, E. 1991 *Modelling biological populations in space and time*. Cambridge University Press.
Rhodes, B. & Anderson, R. M. 1996 Power laws governing epidemics in isolated populations. *Nature* **381**, 600–602.
Ricklefs, R. E. & Schulter, D. (eds) 1993 *Species diversity in ecological communities*. University of Chicago Press.
Rosenzweig, M. L. 1995 *Species diversity in space and time*. Cambridge University Press.
Schaffer, W. M. 1984 Stretching and folding in lynx fur returns: evidence for a strange attractor in nature? *Am. Nat.* **124**, 798–820.
Schaffer, W. M. 1985 Order and chaos in ecological systems. *Ecology* **66**, 93–103.
Sneppen, K. & Newman, M. E. J. 1997 Coherent noise scale invariance and intermittency in large systems. *Physica* D **110**, 209–222.
Solé, R. V. & Goodwin, B. C. 2001 *Signs of life: how complexity pervades biology*. New York: Perseus Books.
Solé, R. V., Manrubia, S. C., Luque, B., Delgado, J. & Bascompte, J. 1996 Phase transitions and complex systems. *Complexity* **1**, 13–26.
Solé, R. V., Manrubia, S. C., Kauffman, S. A., Benton, M. & Bak, P. 1999 Criticality and scaling in evolutionary ecology. *Trends Ecol. Evol.* **14**, 156–160.
Solé, R. V., Alonso, D. & McKane, A. 2000 Scaling in a network model of a multispecies ecosystem. *Physica* A **286**, 337–344.
Stanley, H. E. (and 11 others) 1996 Scaling and universality in animate and inanimate systems. *Physica* A **231**, 20–48.
Tilman, D. 1994 Competition and biodiversity in spatially structural habitats. *Ecology* **75**, 2–16.
Tilman, D., May, R. M., Lehman, C. L. & Nowak, M. A. 1994 Habitat destruction and the extinction debt. *Nature* **371**, 65–66.
Turchin, P. & Ellner, S. P. 1998 Time-series modeling of population fluctuations. In *Chaos in real data: analysis of nonlinear dynamics from short ecological time-series* (ed. J. N. Perry, R. H. Smith, I. P. Woiwod & D. R. Morse). Dordrecht, The Netherlands: Kluwer.
Van Kampen, N. G. 1981 *Stochastic processes in physics and chemistry*. Amsterdam: Elsevier.
Williams, R. J. & Martinez, N. D. 2000 Simple rules yield complex food webs. *Nature* **404**, 180–183.
Winemiller, K. O. 1990 Spatial and temporal variation in tropical fish trophic networks. *Ecol. Monogr.* **60**, 331–367.
Wright, S. 1931 Evolution in Mendelian populations. *Genetics* **16**, 97–159.

GLOSSARY

SAR: species–area relation
SCA: stochastic cellular automata
SOC: self-organized criticality
FFM: forest-fire model
BCT: Bak–Chen–Tang
DS: Drossel–Schwabl
HF: highly fluctuating